



---

# MODELING OF REGENERATIVE CHATTER OF A MILLING PROCESS TO DELINEATE STABLE CUTTING REGION FROM UNSTABLE REGION

**Ezugwu, C. A, Osueke, C. O, Onokwai, A. O, Uguru-Okorie, D. C, Ikpotokin, I and Ibikunle, R**

Department of Mechanical Engineering, College of Engineering, Landmark University  
Omu-Aran, Kwara State. Nigeria

**Olayanju, T.M.A**

Department of Agricultural and Bio-Systems Engineering, College of Engineering,  
Landmark University, Omu-Aran, Kwara State. Nigeria

## ABSTRACT

*This research tries to find a meeting point that will reduce regenerative chatter which is a prolonged form of chatter under control by modeling the machining process using first order least square full discretization method. A mathematical model was developed to assist to locate the productive spindle speed at which the lobbing effects occur and depth of cut combination for the machinist. Computational algorithm was developed for the purpose of delineating stability lobe diagram into stable and unstable regions. The results show considerably smooth milling which will be of immense benefit to machinist in choosing the route to follow in machining oppression.*

**Keywords:** Full discretization, delineate, milling, model, regenerative.

**Cite this Article:** Ezugwu, C. A, Osueke, C. O, Onokwai, A. O, Olayanju, T.M.A, Uguru-Okorie, D. C, Ikpotokin, I and Ibikunle, R, Modeling of Regenerative Chatter of a Milling Process to Delineate Stable Cutting Region from Unstable Region, International Journal of Mechanical Engineering and Technology, 9(11), 2018, pp. 748–757.

<http://www.iaeme.com/IJMET/issues.asp?JType=IJMET&VType=9&IType=11>

---

## 1. INTRODUCTION

Milling is an intermittent process which involves the removal of material by engagement of workpiece pass a spinning multi-tooth cutter as can be seen in metal, wood, ceramics, glass. etc.[1]. It forms a dominant part of a machining process in manufacturing technology with its use spanning cross machining of die, mould and complex aerospace parts [2]. Efficiency of milling process is shortchanged by vibration which itself is triggered off by machining

conditions. Chatter vibration is a product of dynamic robs off between the tool and the workpiece in a milling process under unstable cutting parameters combination [3, 4].

As there is relative motion between tool and work piece, various internal and external forces rises in tool and work piece. These forces set up vibration in machine part which is in motion or at rest. Basically three types of vibration occur in machine, free vibration, forced vibration and self-excited vibration [5]. First two vibrations can be easily detected and controlled by using dampers and by other means. But, mainly chatter prediction is major task for the operator while operating at higher speed [6].

Basically, milling is classified into peripheral milling and face milling as seen in Figure 1. Peripheral milling results in a surface that is parallel to the tool axis and it's usually implemented on a horizontal milling machine, hence, alternative name "Horizontal milling".

Face milling produces a surface that is at right angle with the tool axis and it's usually implemented on vertical milling machines, hence, alternative name "vertical milling"[3].

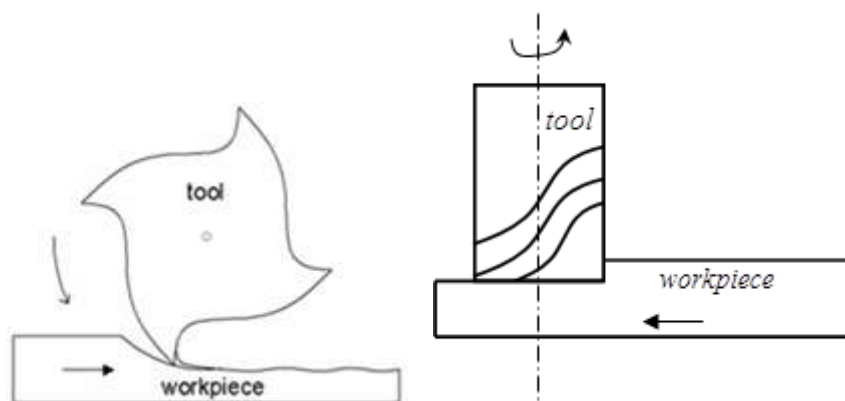


Figure 1 (a) Peripheral Milling (b) Face Milling.

## 2. THE MATHEMATICAL MODEL OF MILLING PROCESS

The two degree of freedom milling model is considered more realistic being that real tools lack rigidity in transverse plane causing compliance in both the feed and feed-normal directions. The two degree of freedom model of flexible milling tool cutting a rigid workpiece as presented by Insperger and Stepan [7].

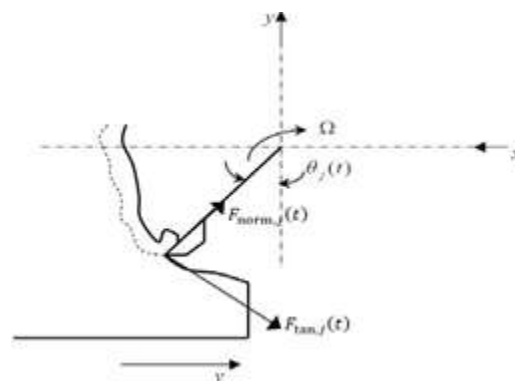


Figure 2 Milling tooth workpiece disposition

The cutting forces on  $j$ th tooth are given by the non-linear law as follows

$$F_{t,j}(t) = c_t w [f_a \sin \theta_j(t)]^y \quad (1)$$

$$F_{n,j}(t) = c_n w [f_a \sin \theta_j(t)]^y = x F_{t,j}(t) \quad (2)$$

The symbols  $C_t$  and  $C_n$  are the tangential and normal cutting coefficients which are numerically influenced by workpiece material properties and tool shape. The symbol  $N$  stands for the number of tool teeth. Where  $w$  is the depth of cut,  $x$  is the ratio of  $c_n/c_t$ ,  $f_a$  is the actual feed given as  $x(t) - x(t - \tau)$  which is the difference between present and one period delayed position of tool and  $\gamma$  is an exponent that is usually less than one, having a value of  $\frac{3}{4}$  for the three-quarter rule. The instantaneous angular position of  $j$ th tooth  $\theta_j(t)$  is given as

$$\theta_j(t) = \left(\frac{\pi\Omega}{30}\right)t + (j - 1)\frac{2\pi}{N} + \alpha \quad (3)$$

The dynamical model shown in Figure 3 is a 2 DOF depiction of an end-milling tool that vibrates in the  $x - y$  plane (horizontal plane). The modal parameters  $k_x, m_x$  and  $c_x$  are for  $x$  -vibration while  $k_y, m_y$  and  $c_y$  are for  $y$  -vibration

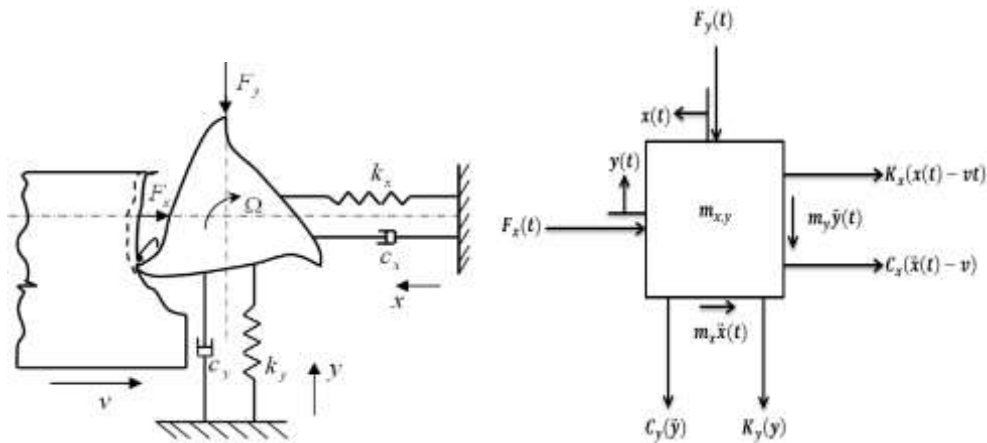


**Figure 3** (a) 2-DOF tool dynamics (b) Free-body diagram of tool dynamics.

Adapted from [6]

The governing equation of motion now becomes

$$m_x \ddot{x}(t) + c_x [\dot{x}(t) - v] + k_x [x(t) - vt] + F_x x(t) = 0 \quad (4)$$

$$m_y \ddot{y}(t) + c_y \dot{y}(t) + ky(t) + F_y(t) = 0 \quad (5)$$

It can be deduce from figure 3 that the  $x$  and  $y$  -component of the cutting force on the tool are

$$F_x(t) = \sum_{j=g_j}^N [F_{n,j}(t) \sin\theta_j(t) + F_{t,j}(t) \cos\theta_j(t)] \quad (6)$$

$$F_y(t) = \sum_{j=g_j}^N [-F_{n,j}(t) \cos\theta_j(t) + F_{t,j}(t) \sin\theta_j(t)] \quad (7)$$

The actual feed rate  $f_a$  of  $j$ th tooth at angular position  $\theta_j(t)$  from Figure 3 are

$$f_a(t) = [X(t) - x(t - \tau)] \sin\theta_j(t) + [Y(t) - y(t - \tau)] \cos\theta_j(t) \quad (8)$$

where  $X(t) = vt + x_t(t) + x(t), Y(t) = y_t(t) + y(t)$

The quantity  $x(t)$  and  $y(t)$  are perturbations in the  $x$  and  $y$  -directions respectively.

The linearized Taylor series expansion of  $f_a^\gamma$  about  $vt \sin\theta_j(t)$  then reads

$$f_a^\gamma = [vt \sin\theta_j(t)]^\gamma + \gamma [vt \sin\theta_j(t)]^{\gamma-1} \{ [x(t) - x(t - \tau)] \sin\theta_j(t) + [y(t) - y(t - \tau)] \cos\theta_j(t) \} \quad (9)$$

Setting  $x(t)$  and  $y(t)$  to zero in equations (9), (1-2) and (6-7) above will lead to the formation of equations (10) and (11) from equations (4) and (5)

$$m_x \ddot{x}(t) + c_x \dot{x}_t(t) + k_x x_t(t) = -F_{px}(t) \quad (10)$$

$$m_y \ddot{y}(t) + c_y \dot{y}_t(t) + k_y y_t(t) = -F_{py}(t) \quad (11)$$

Where

$$F_{px}(t) = cw(v\tau)^y \sum_{j=g_j}^N \sin^y \theta_j(t) [x \sin \theta_j(t) + \cos \theta_j(t)] \quad (12)$$

$$F_{py}(t) = cw(v\tau)^y \sum_{j=g_j}^N \sin^y \theta_j(t) [-x \cos \theta_j(t) + \sin \theta_j(t)] \quad (13)$$

The periodic forces  $-F_{px}(t)$  and  $-F_{py}(t)$  respectively drives the two orthogonal  $\tau$  –periodic tool responses  $x_t(t)$  and  $y_t(t)$ .

Putting equations (10-11) into equation (4-5) and simplifying give

$$m_x \ddot{x}_x(t) + c_x \dot{x}_x(t) + k_x x_x(t) = -h_{xx}(t)[x(t) - x(t - \tau)] - h_{xy}(t)[y(t) - y(t - \tau)] \quad (14)$$

$$m_y \ddot{y}_y(t) + c_y \dot{y}_y(t) + k_y y_y(t) = -h_{yx}(t)[x(t) - x(t - \tau)] - h_{yy}(t)[y(t) - y(t - \tau)] \quad (15)$$

With the specific periodic cutting force variations, we have as

$$h_{xx}(t) = C_t \sum_{j=1}^N g_j(t) \sin(\theta_j(t)) [(C_n/C_t) \sin \theta_j(t) + \cos \theta_j(t)] \quad (16)$$

$$h_{xy}(t) = C_t \sum_{j=1}^N g_j(t) \cos \theta_j(t) [(C_n/C_t) \sin \theta_j(t) + \cos \theta_j(t)] \quad (17)$$

$$h_{yx}(t) = C_t \sum_{j=1}^N g_j(t) \sin(\theta_j(t)) [(C_n/C_t) \cos \theta_j(t) - \sin \theta_j(t)] \quad (18)$$

$$h_{yy}(t) = C_t \sum_{j=1}^N g_j(t) \cos \theta_j(t) [(C_n/C_t) \cos \theta_j(t) - \sin \theta_j(t)] \quad (19)$$

Putting equations (14) and (15) in matrix form gives

$$\ddot{x}(t) + M^{-1}C\dot{x}(t) + M^{-1}Kx(t) = M^{-1}H(t)[x(t) - x(t - \tau)] \quad (20)$$

Where  $X(t) = \{x(t) \ y(t)\}^T$  is the vector of chatter vibration in the two orthogonal directions of  $x$  and  $y$ , the mass  $M$ , damping  $C$  and stiffness  $K$  matrices are respectively given as

$$M = \begin{bmatrix} m_x & 0 \\ 0 & m_y \end{bmatrix}, C = \begin{bmatrix} c_x & 0 \\ 0 & c_y \end{bmatrix}, K = \begin{bmatrix} k_x & 0 \\ 0 & k_y \end{bmatrix} \quad (21)$$

The forcing function in equation (21)  $H(t)X(t - \tau)$  contains a time-periodic function  $H(t)$  that results from rotational motion of the milling teeth

$$H(t) = -w \begin{bmatrix} h_{xx}(t) & h_{xy}(t) \\ h_{yx}(t) & h_{yy}(t) \end{bmatrix} \quad (22)$$

The subscripts in equation (21) indicate the direction of tool modal parameters as shown in figure 3.

It is seen that the performance prescription parameters of interest in this work namely;  $w$  and  $b$  are contained the governing model (equation (20)) via  $H(t)$  and  $g_j(t)$  respectively and thus could be studied simultaneously. By pre-multiplying equation (20) with the inverse of the mass matrix, the modal form of the governing model upon little re-arrangement becomes

$$\ddot{x}(t) + M^{-1}C\dot{x}(t) + M^{-1}[K - H(t)]x(t) = -M^{-1}H(t)x(t - \tau) \quad (23)$$

The expanded form of equation (23) when each of the matrix operations  $M^{-1}C$ ,  $M^{-1}K$  and  $M^{-1}[K - H(t)]$  are carried out reads

$$\begin{Bmatrix} \ddot{x}(t) \\ \ddot{y}(t) \end{Bmatrix} + \begin{bmatrix} 2\zeta_x\omega_{nx} & 0 \\ 0 & 2\zeta_y\omega_{ny} \end{bmatrix} \begin{Bmatrix} \dot{x}(t) \\ \dot{y}(t) \end{Bmatrix} + \begin{bmatrix} \omega_{nx}^2 + \frac{wh_{xx}(t)}{m_x} & \frac{wh_{xy}(t)}{m_x} \\ \frac{wh_{yx}(t)}{m_y} & \omega_{ny}^2 + \frac{wh_{yy}(t)}{m_y} \end{bmatrix} \begin{Bmatrix} x(t) \\ y(t) \end{Bmatrix} = \begin{bmatrix} \frac{wh_{xx}(t)}{m_x} & \frac{wh_{xy}(t)}{m_x} \\ \frac{wh_{yx}(t)}{m_y} & \frac{wh_{yy}(t)}{m_y} \end{bmatrix} \begin{Bmatrix} x(t-\tau) \\ y(t-\tau) \end{Bmatrix} \quad (24)$$

Equation (24) above is the modeled equation for milling chatter whose stability behaviour will be used to predicts a milling process.

### 3. CONCEPT OF STABILITY ANALYSIS OF A MILLING PROCESS

Looking at the governing model (equation (24)), four state variables can be identified;  $x(t)$ ,  $y(t)$ ,  $\dot{x}(t)$  and  $\dot{y}(t)$ . The state variables are then designated as follows;  $y_1(t) = x(t)$ ,  $y_2(t) = y(t)$ ,  $y_3(t) = \dot{x}(t)$  and  $y_4(t) = \dot{y}(t)$ .

$$\dot{y}(t) = \mathbf{A}(t)y(t) - \mathbf{B}(t)y(t - \tau) \quad (25)$$

Where  $y(t) = \{y_1(t) \ y_2(t) \ y_3(t) \ y_4(t)\}^T$  (the superscript ‘‘T’’ means transposition)

$$\mathbf{A}(t) = \begin{bmatrix} 0 & 0 & 1 & 0 \\ 0 & 0 & 0 & 1 \\ -\omega_{nx}^2 - \frac{wh_{xx}(t)}{m_x} & -\frac{wh_{xy}(t)}{m_x} & -2\zeta_x\omega_{nx} & 0 \\ -\frac{wh_{yx}(t)}{m_y} & -\omega_{ny}^2 - \frac{wh_{yy}(t)}{m_y} & 0 & -2\zeta_y\omega_{ny} \end{bmatrix} \quad (26)$$

$$\mathbf{B}(t) = \begin{bmatrix} 0 & 0 & 0 & 0 \\ 0 & 0 & 0 & 0 \\ -\frac{wh_{xx}(t)}{m_x} & -\frac{wh_{xy}(t)}{m_x} & 0 & 0 \\ -\frac{wh_{yx}(t)}{m_y} & -\frac{wh_{yy}(t)}{m_y} & 0 & 0 \end{bmatrix} \quad (27)$$

Re-arrangement of equation (25) which is the needed governing model to conform with the full-discretization method entails splitting the matrix  $\mathbf{A}(t)$  into  $\mathbf{B}(t)$  and a constant matrix  $\mathbf{A}$  such that equation (25) becomes

$$\dot{y}(t) = \mathbf{A}y(t) + \mathbf{B}(t)y(t) - \mathbf{B}(t)y(t - \tau) \quad (28)$$

where

$$\mathbf{A} = \begin{bmatrix} 0 & 0 & 1 & 0 \\ 0 & 0 & 0 & 1 \\ -\omega_{nx}^2 & 0 & -2\zeta_x\omega_{nx} & 0 \\ 0 & -\omega_{ny}^2 & 0 & -2\zeta_y\omega_{ny} \end{bmatrix} \quad (29)$$

The model of milling adopted in this work is the usual procedure which involves discretizing the system’s period and interpolating or approximating the solution in the discrete intervals. The full-discretization method is the choice of stability analysis in this work because it has been proven to clearly draw a line or boundary for classification of milling process into stable and unstable than the semi-discretization method[7]. This is due to the introduction of interpolation polynomials in the integration scheme of full-discretization method which upon solving produces a discrete map that is used for stability analysis [1]. The full-discretization method is heavily based on discretization.

The solution in the discrete interval  $[t_i, t_{i+1}]$  arises from definite integration between the limits  $t_i$  and  $t_{i+1}$  to become

$$y_{i+1} = e^{A\Delta t} y_i + \int_{t_i}^{t_{i+1}} e^{A(t_{i+1}-s)} [B(s)y(s) - B(s)y(s - \tau)] ds \quad (30)$$

The first order least squares approximation of the state term  $y(s)$  is give thus;

$$y(s) = \{1 \ s\} \left[ \sum_{l=i}^{i+1} \begin{Bmatrix} 1 \\ s_l \end{Bmatrix} \{1 \ s\} \right]^{-1} \sum_{l=i}^{i+1} \begin{Bmatrix} 1 \\ s_l \end{Bmatrix} y_l \quad (31)$$

It should be noted that  $l = i$  and  $l = i + 1$  in the summation signs of equation (32) corresponding to terms at  $t_i$  and  $t_{i+1}$ . This is re-written as

$$y(s) = \{1 \ s\} \left[ \begin{array}{cc} \sum_{l=i}^{i+1} 1 & \sum_{l=i}^{i+1} s_l \\ \sum_{l=i}^{i+1} s_l & \sum_{l=i}^{i+1} s_l^2 \end{array} \right]^{-1} \left\{ \begin{array}{c} \sum_{l=i}^{i+1} y_l \\ \sum_{l=i}^{i+1} s_l y_l \end{array} \right\} \quad (33)$$

$$y(s) = \frac{t_{i+1} y_i - t_i y_{i+1}}{\Delta t} + \frac{-y_i + y_{i+1}}{\Delta t} s \quad (34)$$

If  $t_i = 0$  and  $t_{i+1} = \Delta t$  are substituted into the above equation, then equation (34) can be put in the form

$$y(s) = \frac{1}{\Delta t} (\Delta t - s) y_i + \frac{1}{\Delta t} s y_{i+1} \quad (35)$$

In the same way as above, the delay state  $y(s - \tau)$  and periodic coefficient matrix  $B(t)$  will also give as

$$y(t - \tau) = \frac{1}{\Delta t} (\Delta t - t) y_{i-r} + \frac{1}{\Delta t} t y_{i+1-r} \quad (36)$$

$$B(s) = \frac{1}{\Delta t} (\Delta t - t) B_i + \frac{1}{\Delta t} t B_{i+1} \quad (37)$$

Inserting equations (31), (36) and (37) into equation (30) yields

$$y_{i+1} = F_0 y_i + (G_{11} B_i + G_{12} B_{i+1}) y_i + (G_{12} B_i + G_{13} B_{i+1}) y_{i+1} - (G_{11} B_i + G_{12} B_{i+1}) y_{i-r} - (G_{12} B_i + G_{13} B_{i+1}) y_{i+1-r} \quad (38)$$

The above equation is re-arrange to give

$$y_{i+1} = P_i (F_0 + G_{11} B_i + G_{12} B_{i+1}) y_i - P_i (G_{12} B_i + G_{13} B_{i+1}) y_{i+1-r} - P_i (G_{11} B_i + G_{12} B_{i+1}) y_{i-r} \quad (39)$$

Where

$$P_i = [I - G_{12} B_i - G_{13} B_{i+1}]^{-1} \quad (40)$$

The local discrete map derived from equation (39) is given by [15]

$$\begin{Bmatrix} y_{i+1} \\ y_i \\ y_{i-1} \\ \vdots \\ y_{i+1-r} \end{Bmatrix} = \begin{bmatrix} M_{11}^i & 0 & \cdots & 0 & M_{1r}^i & M_{1,r+1}^i \\ I & 0 & \cdots & 0 & 0 & 0 \\ 0 & I & \cdots & 0 & 0 & 0 \\ \vdots & \vdots & \vdots & \vdots & \vdots & \vdots \\ 0 & 0 & 0 & 0 & I & 0 \end{bmatrix} \begin{Bmatrix} y_i \\ y_{i-1} \\ y_{i-2} \\ \vdots \\ y_{i-r} \end{Bmatrix} \quad (41)$$

The stability matrix for the system becomes [7]

$$\psi = M_{r-1}M_{r-2} \dots \dots M_0 \quad (42)$$

Where

$$M_i = \begin{bmatrix} M_{11}^i & 0 & \dots & 0 & M_{1r}^i & M_{1,r+1}^i \\ I & 0 & \dots & 0 & 0 & 0 \\ 0 & I & \dots & 0 & 0 & 0 \\ \vdots & \vdots & \vdots & \vdots & \vdots & \vdots \\ 0 & 0 & 0 & 0 & I & 0 \end{bmatrix} \quad (43)$$

The nature of eigen-values of the stability matrix is the criterion for stability characterization of milling process. Asymptotic stability requires all the  $2r + 2$  eigen-values of the stability matrix  $\psi$  to exist within the unit circle centred at the origin of the complex plane [8]. Stability boundary of milling process is then a curve that joins the critical parameter combinations at which maximum-magnitude eigen-values of  $\psi$  lie on the circumference of the unit circle [8]. Milling stability lobes are computed with a value of  $r$  that is big enough to guarantee benchmark accuracy.

#### 4. ALGORITHM TO COMPUTE STABILITY LIMIT OF MILLING

Delineation of milling process into stable or unstable occasioned by regenerative chatter can only have a real, physical or numerical reality when the constant parameters (which include tool, prescription and cutting parameters) are known numerically. The knowledge of tool and cutting parameters can stem from either pure experimental analysis or hybrid of experimental and numerical/theoretical analysis [9].

##### 4.1. Algorithm

Stability limits of milling on the plane of axial depth of cut and radial depth of cut at fixed spindle speed is generated by following the algorithm that follows;

- I. Provide the values of tool and cutting parameters. Also provide the approximation parameter  $r$ , the fixed spindle speed, the step and number of steps of computation for both axial and radial depths of cut.
- II. Compute the time-invariant matrix  $A$  and its inverse, the discrete delay or period  $\tau$ , the discrete time step range  $\Delta t = \frac{\tau}{r}$  and the  $F$  and  $G$  matrices.
- III. Chose the first step of axial depth of cut then chose the first step of radial depth of cut. Form discrete time intervals  $[t_i, t_{i+1}]$  where  $i = 0, 1, 2, \dots \dots (r - 1)$  and  $t_i = i \frac{\tau}{r} = i\Delta t = i(t_{i+1} - t_i)$ . At the extremities of the first discrete time interval  $[t_0, t_1]$  compute  $\theta_j(t)$  and utilize it together with the chosen radial depth of cut to compute  $g_j(t)$  then compute  $h_{xx}(t), h_{xy}(t), h_{yx}(t), h_{yy}(t)$  and use the results to form the matrices  $B(t_0)$  and  $B(t_1)$ . Use the  $G$  matrices together with the matrices  $B(t_0)$  and  $B(t_1)$  to form the matrix  $P_0$ . Then form the matrices  $M_{11}^0, M_{1r}^0$  and  $M_{1,r+1}^0$  from the  $G$  matrices,  $F_0, B(t_0)$  and  $B(t_1)$  and  $P_0$ . Making use of the matrices  $M_{11}^0, M_{1r}^0$  and  $M_{1,r+1}^0$  form the matrix  $M_0$ .
- IV. With the axial depth of cut fixed at value in step4 carry out the operation in the algorithm step4  $r - 1$  times at the remaining steps  $i = 1, 2, \dots \dots (r - 1)$  and use result of all the steps to form the stability matrix  $\psi$ . Compute the eigen-values of  $\psi$  and chose the eigen-value with maximum magnitude.
- V. Repeat steps 3 and 4 for the remaining steps of radial depth of cut.

- VI. Repeat steps 3-6 for the remaining steps of axial depth of cut.
- VII. Connect the parameter combinations of axial and radial depths of cut at which maximum magnitude of eigen-values are unity to form the stability limit.

The algorithms above will be utilized to generate stability limits that will be jointly used to delineate the stability lobes diagram.

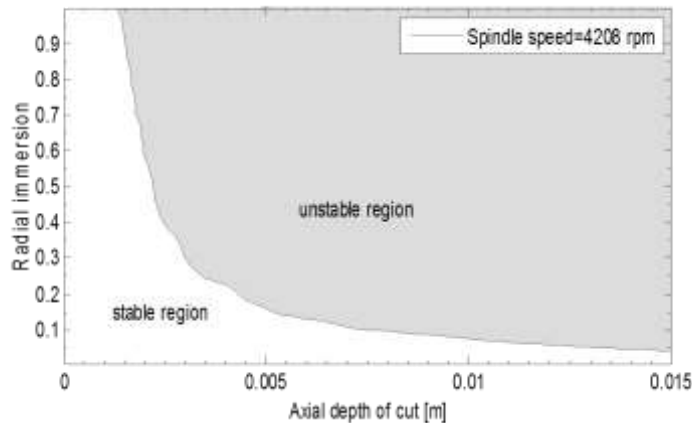
## 5. RESULTS AND DISCUSSION

Utilization of the algorithm in section 4 would enable us generate stability limit that allows selection of the maximum product  $w\rho$ . The graphs of the aforementioned algorithm are mapped out with MATLAB for stability milling process on three different plane of parameter space for comparative analysis [10, 11]. Numerical values of parameters of table 1 are borrowed from Weck et al as cited in [3] and are as presented in table below.

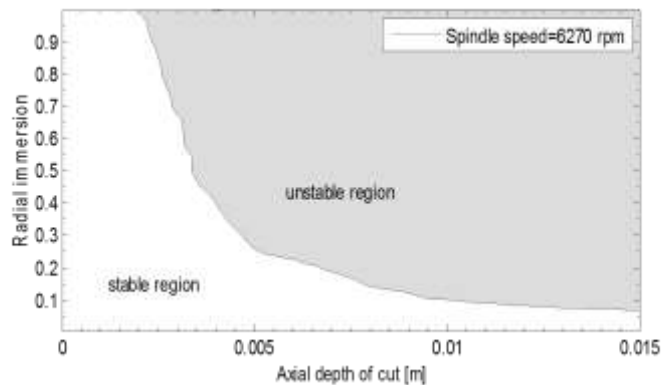
**Table 1** Numerical parameters for milling process stability analysis from

$\omega_{nx}$	600 Hz
$\omega_{ny}$	660 Hz
$k_x$	5600 kN/m
$k_y$	5600 kN/m
$\zeta_x$	0.035
$\zeta_y$	0.035
$m_x$	$k_x/\omega_{nx}^2$
$m_y$	$k_y/\omega_{ny}^2$
<b>N</b>	3
$C_t$	600 mPa
$C_n$	0.07 mPa
$\theta_s$	0 (up-milling)
	Weck et al as cited in [3]

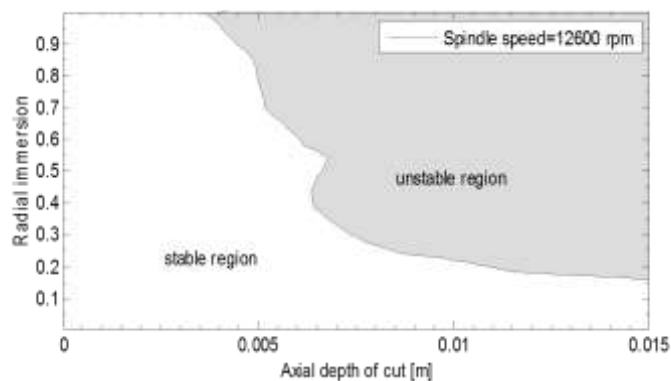
The parameters in table 1 and the algorithm in section 4 were used to generate stability limits of milling process on the plane of axial depth of cut and radial depth of cut at some elected productive speeds of 4208, 6270, 12600 as can be seen below.



(a)



(b)



(c)

**Figure 4** Stability limits of milling on the plane of axial depth of cut and radial depth of cut at selected productive spindle speeds seen in the legends.

It can be seen from the above figure that rise in spindle speed enhances the stable region and suppresses the unstable region. Figure 4c agrees closely with figure generated with identical set of parameters in the work of Tekeli, A. and E. Budak [3]. This meaning that algorithm in section 4 for the first order least square approximated map of the work of Ozoegwu, C.G. [8] provides reliable stability limit of milling process on the plane of depths of cut.

The importance of implementing the algorithm is section 4 for generating stability limit on plane of axial and radial depths of cut need not to be overemphasized when the algorithm is implemented at a non-productive spindle speed of 9000rpm with all other parameters of computation fixed at a value used in generating figure 4c.

## 6. CONCLUSION

Regenerative chatter is a major obstacle to machine administrator this days in accomplishing high accuracy and satisfactory surface finish. There are different methods of controlling regenerative chatter in milling process. These are analytical, semi-analytical while others are experimental. This work establishes the framework for utilization of the least squares approximated full-discretization technique in stability analysis on the plane of axial depth of cut and radial depth of cut analytical method. A point by point computational calculation was displayed for the purpose of delineating the lobes into stable and unstable regions. With the proper understanding of the stability lobe diagram, operators will have fewer factors to

contend with while performing their works because it will specify the exact route to be followed while machining so as to avoid regenerative chatter.

## REFERENCES

- [1] Ezugwu, C.A.K. Minimizing Pocketing Time by Programmed Optimal Choice of Stable Milling Process Parameters: Master of Engineering Thesis, Nnamdi Azikiwe University, Awka, 2015.
- [2] Hashimoto, M., Marui, E., and Kato, S. Experimental research on cutting force variation during regenerative chatter vibration in a plain milling operation. *International Journal of Machine Tools and Manufacture*, 36 (10), 1996, pp. 1073–1092.
- [3] Tekeli, A. and E. Budak, Maximization of chatter-free material removal rate in end milling using analytical methods, *Machining Science and Technology*, 9, 2005, pp. 147–167
- [4] Quintana, G. and Ciurana, J. Chatter in machining processes: a review, *International Journal of Machine Tools and Manufacture*. *International Journal of Machine tools and manufacture*, 51 (5), 2011, pp. 363–376
- [5] J.Tlusty, M.Polacek, “The stability of machine tools against self-excited vibrations in machining”, *International Research in Production Engineering*, 1963, pp.465–474.
- [6] Budak, E., and Altintas, Y. Analytical Prediction of Chatter Stability in Milling - Part I: General Formulation, Part II: Application To Common Milling Systems. *Trans. ASME Journal of Dynamic Systems, Measurement and Control*, 20, 1998, pp. 22–36.
- [7] Insperger T, Stepan G (2004) Updated semi-discretization method for periodic delay differential with discrete delay. *Int J Numer Methods Eng* 61, 2004, pp. 117–141
- [8] Ozoegwu, C.G. Least squares approximated stability boundaries of milling process, *International Journal of Machine Tools and Manufacture*, 79, 2014, pp. 24–30.
- [9] Kalpakjian, S. and Schmidt, S. R. (2003). *Manufacturing Processes for Engineering Material*, 4th Edition. New York; Prentice Hall Publishing Co., 2003, pp. 112-157.
- [10] Okonkwo U. C., Okokpuije I. P., Sinebe J. E., and Ezugwu C. A (2016). Comparative analysis of aluminum surface roughness in end-milling under dry and minimum quantity lubrication (MQL) conditions. *Manufacturing Rev*, 2 (30), 2015. DOI: <http://dx.doi.org/10.1051/mfreview/201503>
- [11] Choi BK, Park SC. (1999). A pair-wise offset algorithm for 2d point-sequence curve. *Computer-Aided Design*, 31(12), 1999, pp. 735–45.